Available online at www.sciencedirect.com
ScienceDirect
Catalysis Today 133–135 (2008) 261–266
CATALYSIS TODAY
www.elsevier.com/locate/cattod

Preparation of highly active NiMo/Al-SBA15 (*x*) HDS catalysts: Preservation of the support hexagonal porous arrangement

Gabriela Macías, Jorge Ramírez *, Aída Gutiérrez-Alejandre, Rogelio Cuevas

UNICAT, Departamento de Ingeniería Química, Facultad de Química, UNAM, Cd. Universitaria, México 04510, D.F., Mexico

Available online 19 February 2008

Abstract

Synthesis, characterization and catalytic evaluation of NiMo HDS catalysts supported on pure and alumina-modified SBA-15 were carried out. For the synthesis of supported-NiMo catalysts, a molybdenum precursor acidic solution and aqueous nickel nitrate solution were used. Mo/SBA-15 catalyst was prepared as reference with an aqueous ammonium heptamolybdate solution. In this case, the support structure is partially destroyed since the heptamolybdate anions react with the pore walls. In contrast, when an acidic solution is used, the formation of a different molybdenum precursor (presumably MoO_2Cl_2), which does not react easily with silica is favored. The catalytic activity test showed that aluminum incorporation in the support framework enables the 4,6-DMDBT HDS reaction mainly by direct desulfurization pathway, probably due to previous isomerization of the molecule by Al-SBA-15 (*x*) acid sites.

Keywords: Al-SBA-15; Hydrodesulfurization; NiMo catalysts; 4,6-DMDBT

1. Introduction

In 1998, Zhao et al. [1,2] employed triblock copolymer surfactants to template the formation of mesoporous silica with different ordered porous structures under highly acidic conditions. Hexagonally ordered SBA-15 is the most outstanding member in the group of templated materials by triblock copolymers due to its easy synthesis, adjustable pore size (from 50 to 300 Å), thick pore walls and notable hydrothermal stability.

Pure silica molecular sieve materials have an electrically neutral framework and thus they lack acidic sites [3–5]. To generate surface acidity in SBA-15, much effort has been directed to the introduction of aluminum into silica network [6–10].

SBA-15 is a pure silica phase prepared in a highly acidic medium (HCl solution 2M) [1]. Since most of aluminum sources dissolve in highly acidic mediums, the precipitation needed for aluminum incorporation into the network seems impossible. Previous studies have shown that aluminum can be effectively incorporated on silica SBA-15 materials through post-synthetic procedures by chemical grafting on the pore wall surface with anhydrous $AlCl_3$ [11], aluminum isopropoxide in non-aqueous solutions [12], or sodium aluminate in aqueous solution [13], followed by calcination.

With the evolution of mesoporous materials, the interest in the application of catalytic active phases onto their pores has grown. Due to more stringent legislations about sulfur specifications in transport fuels, development of new catalysts is required. In this order, it has been attempted to take advantage of the unique textural properties of mesoporous materials to improve the dispersion of cobalt or nickel promoted MoS_2 HDS catalysts [14–18]. Unfortunately, information about support stability after molybdenum precursor impregnation and about the resultant catalyst is scarce. The most common precursor material employed for alumina supported catalysts is ammonium heptamolybdate (AHM). However, it has been shown that pure silica MCM-41 support is structurally and texturally unstable when AHM impregnation procedure is used [19], indicating that this method is not feasible for preparation of MoO_3/MCM-41 catalysts, due to the almost complete support destruction during molybdenum impregnation.

Lensveld [20] reported the preparation of a new molybdenum precursor in acidic medium that does not destroy MCM-41 structure. This precursor, which is conceived as MoO_2Cl_2, was prepared via AHM addition to 1:1 proportion demineralized water–chlorhydric acid mixture. Iler collected data about

* Corresponding author. Tel.: +55 5622 5349; fax: +55 5622 5366.
E-mail address: jrs@servidor.unam.mx (J. Ramírez).

0920-5861/$ – see front matter © 2007 Elsevier B.V. All rights reserved.
doi:10.1016/j.cattod.2007.12.079

solubility of amorphous silica at different pH conditions [21]. It was demonstrated that amorphous silica is soluble in acidic conditions; although the concentration of dissolved silica (at equilibrium) is relatively low, especially at room temperature. It is expected then that SBA-15 materials will behave similarly to MCM-41 concerning the impregnation of Mo in acidic conditions; it will be possible to prepare highly dispersed Mo/SBA-15 catalysts without destroying the support structural order.

The objective of this work is the synthesis and characterization of NiMo HDS catalysts supported on pure and alumina-modified SBA-15 prepared via a molybdenum acidic precursor solution. The catalysts will be tested in the 4,6-DMDBT HDS reaction.

2. Experimental

2.1. Support preparation

SBA-15 was synthesized according to the method reported by Zhao et al. [1]. For the preparation of aluminum-modified SBA-15 supports, the required amount of SBA-15 was dispersed in 300 ml of anhydrous hexane (Aldrich 95+%) containing different amounts of aluminum isopropoxide (AIP, Aldrich 98+%). The resultant mixture was stirred at room temperature during 12 h, and the obtained powder was washed with anhydrous hexane, air dried at room temperature and finally calcined at 823.15 K during 5 h. The synthesized supports were labeled Al-SBA15 (x) where x represents the atomic Si:Al ratio ($x = 30$, 15).

2.2. Catalysts preparation (pH ∼ 0)

Molybdenum precursor solutions were prepared dissolving the required ammonium heptamolybdate amount (AHM, Aldrich ACS Reagent) in a 1:1 demineralized water–concentrated hydrochloric acid (Aldrich 37%) mixture (pH ∼ 0). Before impregnation, supports were dried under vacuum at least 15 min at room temperature. Supports were impregnated by wetness impregnation method with molybdenum precursor solutions. After that, they were dried 12 h at 393.15 K and calcined in air at 723.15 K during 6 h, using a heating ramp of 1 K min^{-1}. In every case the catalyst loading was 12 wt% MoO_3. Mo/SBA-15 was prepared as reference catalyst using the appropriate amount of an AHM aqueous solution (pH 5). This catalyst was dried 24 h at 373.15 K and calcined at 723.15 K during 4 h.

Ni promoter was added by successive impregnation on supported-Mo catalysts with an aqueous solution of nickel nitrate (Baker 99%) in the required amount to obtain 3 wt% as NiO. The catalysts were dried in air at 393.15 K during 12 h and calcined 4 h at 723.15 K (heating rate 1 K min^{-1}).

2.3. Supports and catalysts characterization

Textural properties were obtained from nitrogen adsorption–desorption isotherms measured at 77 K (liquid nitrogen boiling point) with an automatic Micromeritics Tri-Star 3000 analyzer. Before N_2 physisorption, the samples were outgassed 3 h at 543.15 K. X ray diffraction patterns were recorded on a Phillips PW 1050/25 powder diffraction system using Cu Kα radiation with Ni filter ($\lambda = 1.5406$ Å) over $3^\circ \leq 2\Theta \leq 90^\circ$ (1° (2Θ) min^{-1}) and $0.5^\circ \leq 2\Theta \leq 8^\circ$ (0.5° (2Θ) min^{-1}) ranges. ^{27}Al MAS NMR spectra were recorded on a Bruker Advance 400 equipment, using $Al(H_2O)_6^{3+}$ as external ^{27}Al reference. Determinations were carried out at 300 K with a 104 MHz frequency, spin rate of 9 kHz and 0.5 s delayed recycling. FT-Raman spectra were recorded at room temperature on a Nicolet 950 FT-Raman spectrometer equipped with InGaAs detector and Nd:YAG laser source with resolution of 4 cm^{-1} and 200 scans. For the NO adsorption experiments, a thin wafer of the pure powder was made (8 mg/cm^2) and placed into a special IR cell and sulfided at the same conditions as for catalytic test. Then it was pretreated under vacuum at 773 K for 1 h. After that, a pulse of NO was introduced (56 Torr) at room temperature. IR spectra were collected outgassing at room temperature and at 373 K. All experiments were recorded using a Nicolet IR-Magna 760 spectrometer with 4 cm^{-1} of resolution and 100 scans per spectrum.

2.4. Catalytic evaluation

Prior to the catalytic test the oxide catalysts were sulfided 4 h at 673.15 K in a 15% H_2S/85% H_2 mixture (25 ml min^{-1}). 4,6-DMDBT HDS reaction was carried out in a Parr batch reactor with 40 ml of a 4,6-DMDBT-decane solution (1000 ppm S) at 573.15 K and 1000 psia. Reaction products were analyzed on a HP 6890 Gas Chromatograph equipped with a 50 m length × 0.2 mm diameter × 0.5 μm film thickness capillary column.

3. Results and discussion

3.1. Mo/SBA-15 catalysts

Fig. 1 shows low angle $2\theta = 0.75$–2.5 range diffractograms of Mo catalysts prepared in acidic (pH ∼ 0) and aqueous (pH 5) conditions. It is evident from the intensity of the (1 0 0) reflection that for samples prepared in aqueous conditions SBA-15 structure is deteriorated; while in acidic conditions the support structure is preserved. As regards the $2\theta = 5$–85 range diffractograms (see insert, Fig. 1), using AHM aqueous precursor enhances the formation of MoO_3 crystalline species suggesting low dispersion. On the other hand, MoO_3 species were not detected when impregnation was carried out at acidic conditions.

Fig. 2 shows the adsorption–desorption isotherms of catalysts. Mo catalysts synthesized under aqueous conditions present a slight enlargement of the capillary condensation region suggesting partial destruction of the mesoporous SBA-15 structure; this effect does not occur under acidic conditions. In every case a narrow pore size distribution with maximum at 65 Å is observed. Based on these results, the catalysts were prepared using acidic conditions. The precursor formed at

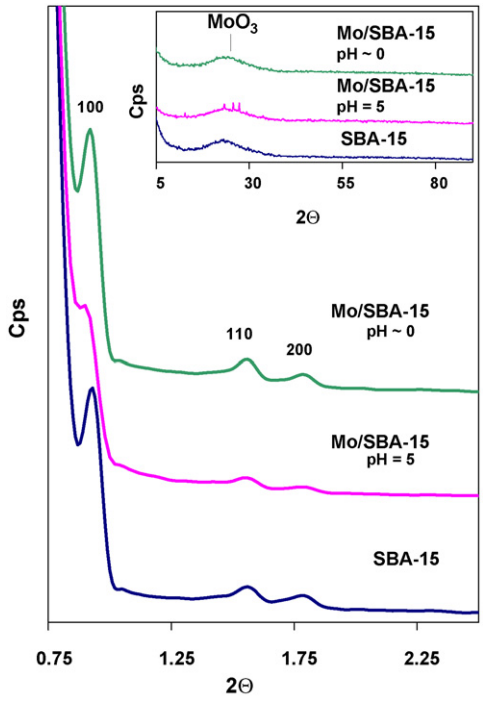

Fig. 1. Diffractograms of Mo/SBA-15 catalysts prepared at different pH of molybdenum precursor impregnation solution.

acidic pH values is solid MoO_2Cl_2, which quickly hydrolyzes in contact with water [22–24], due to the equilibrium:

$$MoO_2Cl_2 + H_2O \leftrightarrow MoO_3 + 2HCl \quad (1)$$

At sufficiently high HCl concentration, MoO_2Cl_2 is a thermodynamically stable species [24], which practically does

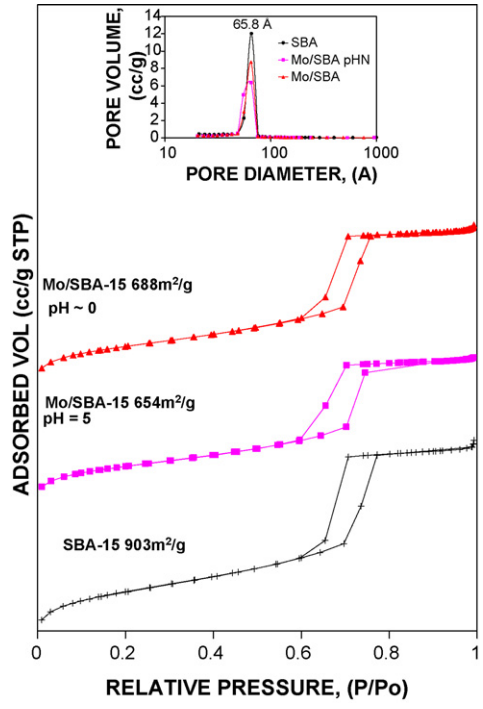

Fig. 2. Nitrogen adsorption–desorption isotherms and pore volume distribution of Mo/SBA-15 catalysts prepared at different pH of molybdenum precursor impregnation solution.

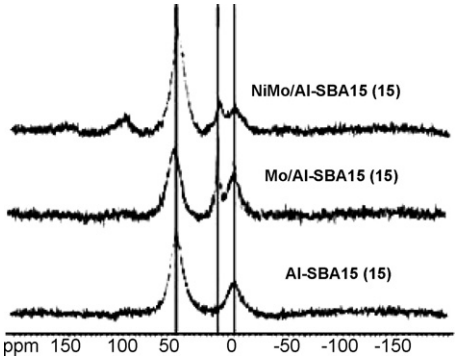

Fig. 3. ^{27}Al MAS NMR spectra of NiMo catalysts supported on Al-SBA15 (15) series.

not react with silica. In the case of impregnation with the aqueous AHM solution at pH 5, $Mo_7O_{24}^{6-}$ isopoly-anions are present in solution. These (poly)molybdate anions interact with silica, giving rise to the formation of heteropoly-anions [25,26].

$$12Mo_7O_{24}^{6-} + 7SiO_2 + 22H_2O \leftrightarrow 7SiMo_{12}O_{40}^{4-} + 44OH^- \quad (2)$$

3.2. NiMo/Al-SBA15 (x) catalysts

To analyze the way aluminum interacts with SBA-15 framework, ^{27}Al MAS NMR spectroscopy was used. ^{27}Al MAS NMR spectra of NiMo/Al-SBA15 (*x*) are showed in Figs. 3 and 4. The peak at 50 ppm is assigned to aluminum in tetrahedral environment (structural unit AlO_4), where aluminum is covalently bonded to four silicon atoms via oxygen bridges. The 0 ppm peak is related to octahedral aluminum (structural unit AlO_6) [27]. Results plainly show the existence of both AlO_4 and AlO_6 structural units. However, it is evident when comparing the intensity of these two peaks that AlO_4 concentration is lower than AlO_6, suggesting that most of the grafted aluminum on SBA-15 is tetrahedrally coordinated, indicating that it was incorporated into silica framework.

After molybdenum incorporation (Figs. 3 and 4) a new signal at 10 ppm appears, which can be assigned to "an hydrated form of aluminum molybdate $Al_2(MoO_4)_3$" [28]. It is

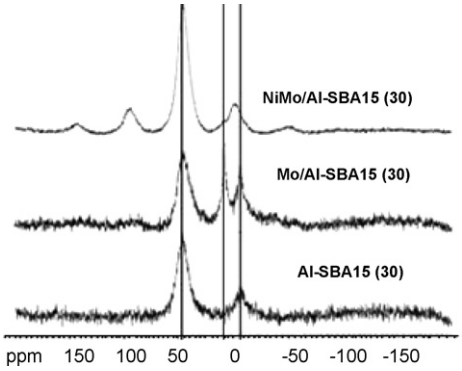

Fig. 4. ^{27}Al MAS NMR spectra of NiMo catalysts supported on Al-SBA15 (30) series.

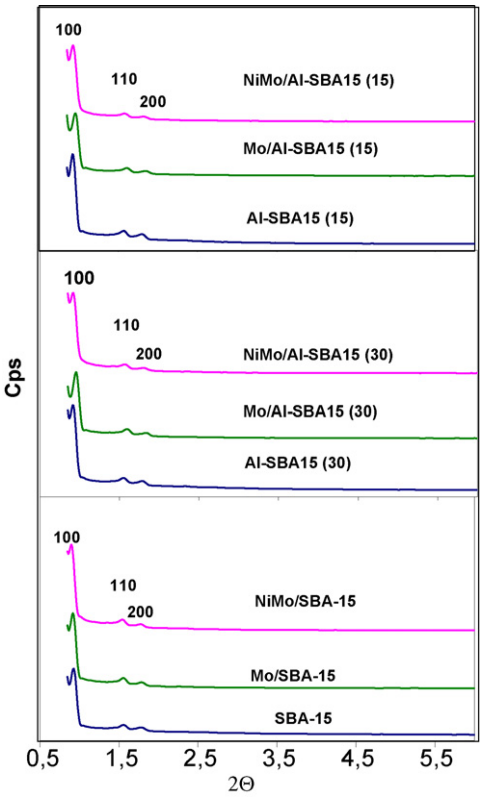

Fig. 5. Diffractograms of catalysts and supports at low angle.

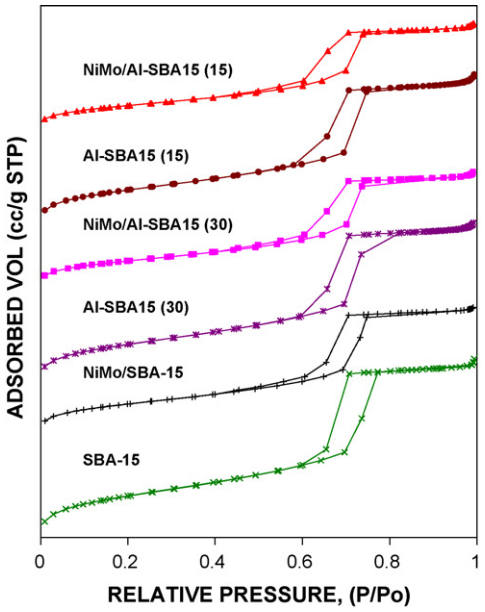

Fig. 6. Nitrogen adsorption–desorption isotherms for supports and NiMo catalysts.

thought that this species is an Anderson type heteropolymolybdate $[Al(OH)_6Mo_6O_{18}]^{3-}$. Formation of this aluminum molybdate ion could be explained through alumina dissolution and the subsequent reaction of dissolved Al^{3+} with AHM during the impregnation step. $Al_2(MoO_4)_3$ could be formed as a result of the interaction of Mo species with "highly reactive" extra-framework aluminum species. However, this peak (10 ppm) disappears when Ni promoter is added, suggesting that its impregnation eliminates the formation of $[Al(OH)_6Mo_6O_{18}]^{3-}$ type compounds and avoids support dealumination.

As shown in Fig. 5, every Mo and NiMo catalysts displays the three well defined characteristic peaks of SBA-15, indexed as (1 0 0) reflection at 0.93°, (1 1 0) at 1.57° and (2 0 0) at 1.8°, associated with the *p6mm* hexagonal symmetry. This indicates that after impregnation of Mo and Ni phases the characteristic hexagonal structure of SBA-15 and Al-SBA15 (*x*) is preserved. Cell parameter a_0 ($a_0 = 2d_{100}/\sqrt{3}$) and d_{100} spacing of every catalyst (Table 1) are very similar to those found in the corresponding supports. In contrast, wall thickness E ($=a_0 - d_{pore}$) increases with molybdenum and nickel precursors impregnation. These data indicate that the hexagonal pore arrangement of the support is not altered after impregnations and that metals cover the walls of the pores increasing their wall thickness. Neither Mo nor Ni crystalline species were detected by XRD suggesting a good dispersion of the metallic phases.

N_2 physisorption isotherms of supports and catalysts (Fig. 6) correspond, according to IUPAC, to a typical irreversible type IV isotherm with H1 hysteresis. SBA-15 isotherm shows an inflection point at $P/P_0 = 0.6$–0.8, characteristic of capillary condensation inside uniform cylindrical pores. P/P_0 position of inflection points is related with a diameter in the mesoporous range and the sharpness of the step indicates uniformity in the pore size distribution. The starting point of the hysteresis is slightly shifted to lower P/P_0 values when aluminum loading is increased, indicating that alumination decreases the surface area and makes SBA-15 pore diameter narrower, probably by aluminum deposition on the SBA-15 pore walls. From Table 1, it can be observed that pore diameter and pore size distribution stay almost constant after impregnation of molybdenum and nickel oxide phases.

Table 1
Physical properties and catalytic activity of NiMo catalysts supported on hexagonal mesoporous materials type SBA-15

	Sg (m^2/g)	d_{100} (Å)	d_{pore} (Å)	a_0 (Å)	E (Å)	X	k (h^{-1})	HYD/DDS	Tol/MCH	CUS-Ni^{2+}/CUS Mo^{4+}
SBA-15	903	94.9	65.8	109.6	43.8	–	–	–	–	–
Al-SBA15 (30)	785	95.9	65.6	110.8	45.2	–	–	–	–	–
Al-SBA15 (15)	708	94.9	65.3	109.6	44.3	–	–	–	–	–
NiMo/SBA-15	596	98.1	64.6	113.3	48.7	69.7	0.197	7.9	1.81	1.75
NiMo/Al-SBA15 (30)	509	95.9	64.1	110.8	46.7	93.5	0.390	4.5	2.16	3.59
NiMo/Al-SBA15 (15)	461	94.9	54.7	109.6	54.9	98.5	0.444	5.1	2.02	5.33

a_0: cell parameter; E: wall thickness; X: 4,6-DMDBT conversion at $t = 6$ h; HYD/DDS: hydrogenation products/direct desulfurization product; Tol/MCH: toluene/methylcyclohexane.

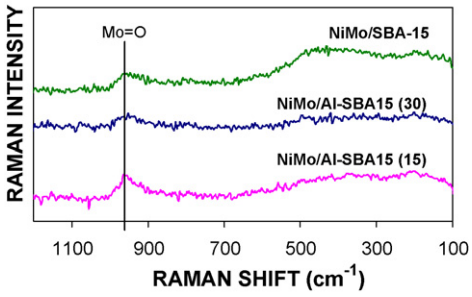

Fig. 7. FT-Raman spectra of NiMo catalysts.

Due to MoO_3 compound generally gives rise to strong Raman signals and those produced by oxide supports like SiO_2 and Al_2O_3 are weak, FT-Raman spectroscopy results a useful characterization technique that provides fundamental information about the surface molybdenum oxide species present in SiO_2–Al_2O_3 supported catalysts. Fig. 7 shows the Raman spectra corresponding to NiMo catalysts. Every spectrum presents a broad band at ~960 cm^{-1}, which is assigned to Mo = O stretching vibrations of monolayer surface Mo species. For NiMo/Al-SBA15 (15), this peak is more intense. The lack of characteristic peaks assigned to crystalline MoO_3 (996, 821, 667 and 285 cm^{-1}) indicates high dispersion of surface molybdenum species.

To enquire on the degree of unsaturation of molybdenum and nickel sites, NO adsorption experiments were conducted on the different sulfided catalysts. For Mo oxide phase, it is reported the existence of two NO infrared bands at 1800–1815 cm^{-1} and 1700–1715 cm^{-1} related to symmetric and antisymmetric N–O stretching vibration mode respectively. In sulfided state, these bands appear shifted toward lower wavenumbers by a maximum of 40 cm^{-1} [29]. Fig. 8 shows NO adsorption FTIR spectra of NiMo catalysts. The bimetallic catalysts exhibit two Mo associated bands at 1690 and 1810 cm^{-1} and one additional at 1855 cm^{-1}, which is associated with CUS-Ni^{2+} sites. The 1855–1690 cm^{-1} band intensity ratio gives and idea about proportion of coordinatively unsaturated sites or CUS (CUS-Ni^{2+}/CUS-Mo^{4+}) and their value is presented in Table 1. The value of the CUS-Ni^{2+}/CUS-Mo^{4+} ratio increases with the amount of aluminum incorporated into the support, indicating a higher number of CUS-Ni^{2+} sites possibly associated to MoS_2 crystallites promoted by nickel, as previously reported [30,31].

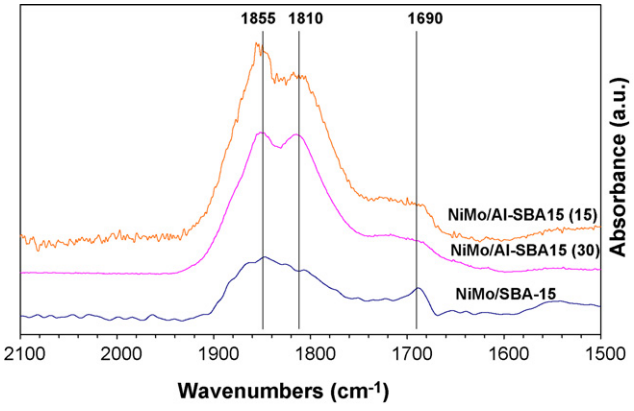

Fig. 8. FTIR spectra of sulfided NiMo/Al-SBA15 (*x*) catalysts after NO adsorption.

In summary, the characterization results indicate that grafted aluminum on SBA-15 is in tetrahedral coordination suggesting that it is incorporated into the silica framework. After Mo and Ni phases impregnation by the method outlined here, the characteristic hexagonal structure of SBA-15 is preserved and neither Mo nor Ni crystalline species are detectable, indicating good dispersion of the metallic phases. Accordingly, surface area and pore diameter of the catalysts are similar to those of the corresponding support. The increase of CUS-Ni^{2+}/CUS-Mo^{4+} ratio suggests molybdenum promotion by nickel when aluminum is incorporated to SBA-15 framework.

3.3. Catalytic activity

Table 1 shows the HDS conversion (*X*) results at $t = 6$ h for 4,6-DMDBT and the values of the pseudo first order reaction rate constant (k, h^{-1}). 4,6-DMDBT percent conversion was defined as (moles of 4,6-DMDBT converted/initial moles of 4,6-DMDBT) × 100. The higher k values correspond to the catalysts supported on alumina-modified SBA-15 and among them NiMo/Al-SBA15 (15) presents the highest conversion. In contrast, the catalyst supported on pure SBA-15 displayed an activity 2.25 times smaller than NiMo/Al-SBA15 (15). These results are in agreement with those obteined by NO adsorption FTIR spectroscopy.

Most of the authors who have performed experiments involving hydrotreatment acidic catalysts, have proposed that the improvement of 4,6-DMDBT transformation, associated to catalyst acidic character, is due to the displacement of methyl groups (isomerization) [32–39]. All the proposed reaction pathways can be summarized in Fig. 9 where the hydrogenation routes have also been included.

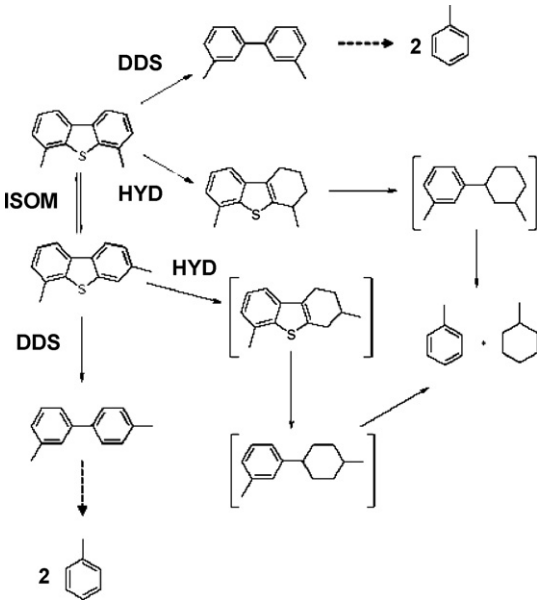

Fig. 9. Reaction scheme of 4,6-DMDBT HDS through HYD and DDS pathways [40].

For the analysis of the reaction pathways, 4,6-dimethyltetrahydrodibenzothiophene (DMTHDBT) and dimethylcyclohexilbenzene (DMCHB) were considered as HYD pathway products, and all dimethylbiphenyls as desulfurization (DDS) products.

The ratio between HYD and DDS products and toluene/methylcyclohexane ratio calculated at $X = 60\%$ are displayed in Table 1. For every catalyst, HYD/DDS ratio is between 5 and 8, which indicates a predominance of the hydrogenation route over hydrodesulfurization one. The fact that the ratio decreases with aluminum content while the overall activity increases substantially, as the rate constants indicate, can be rationalized by either an increase in the DDS routes or a decrease in hydrogenation. Since the route ISOM-DDS increases its contribution with the catalyst acidity, it is likely that the HYD/DDS ratio decrease is due to a greater relative contribution of the ISOM-DDS pathway. The Tol/MCH ratio increases with Al incorporation and is higher than one for all catalysts. Since the hydrogenation route produces equimolar amounts of toluene and MCH, the Tol/MCH ratio higher than one indicates that other route, most likely the ISOM-DDS one is producing extra toluene. It is reported that once 4,6 DMDBT isomerizes the ISOM-DDS route is favored over the ISOM-HYD pathway [40]. So, it appears then that the use of Al-SBA15 materials as supports in NiMo catalysts where Mo is impregnated at pH values close to zero preserves the hexagonal porous arrangement of SBA-15 and renders active HDS catalysts that use the hydrogenation and isomerization pathways to accomplish the hydrodesulfurization of 4,6-DMDBT.

4. Conclusions

It was demonstrated that the synthesis of NiMo catalysts supported on Al-SBA15 using acid Mo precursor solutions avoids molybdenum reaction with mesopores walls leading to preservation of the support hexagonal pore arrangement.

Aluminum incorporation to the surface of SBA-15 increases the transformation of 4,6-DMDBT. The product distribution shows that the increase in activity is due to a greater contribution of the isomerization reaction pathway when aluminum is present on the catalyst. This is consistent with reports indicating increased acidity for Al-modified SiO_2 supports. The improvement in the overall HDS activity was related to the higher number of coordinatively unsaturated nickel sites. These sites could be associated to molybdenum sulfide promoted by nickel (Ni–Mo–S phase).

Acknowledgements

This work was performed with the financial support of CONACYT, DGEP, and PAPIIT IN-101406-DGAPA-UNAM program. The authors would like to acknowledge Cecilia Salcedo Luna (USAI, UNAM) for obtaining XRD patterns and Gerardo Cedillo Valverde (IIM, UNAM) for his help with ^{27}Al MAS NMR experiments.

References

[1] D. Zhao, J. Feng, Q. Huo, N. Melosh, G.H. Fredrickson, B.F. Chmelka, G.D. Stucky, Science 279 (1998) 548.
[2] D. Zhao, Q. Huo, J. Feng, B.F. Chmelka, G.D. Stucky, J. Am. Chem. Soc. 120 (1998) 6024.
[3] R. Mokaya, W. Jones, Chem. Commun. (1997) 2185.
[4] S.K. Jana, T. Kugita, S. Namba, Appl. Catal. A 266 (2004) 245.
[5] R. Mokaya, J. Catal. 193 (2000) 103.
[6] C.Y. Chen, H.X. Li, M.E. Davis, Micropor. Mater. 2 (1993) 17.
[7] R. Schmidt, D. Akporiaye, M. Stöcker, O.H. Ellestad, J. Chem. Soc., Chem. Commun. (1994) 1493.
[8] A. Corma, V. Fornés, M.T. Navarro, J. Pérez-Pariente, J. Catal. 148 (1994) 569.
[9] V. Luca, D.J. MacLachlan, R. Bramley, K. Morgan, J. Phys. Chem. 100 (1996) 1793.
[10] Z. Luan, H. He, C.F. Cheng, W. Zhou, J. Klinowski, J. Phys. Chem. 99 (1995) 1018.
[11] R. Ryoo, S. Jun, J.M. Kim, M. Kim, J. Chem. Commun. (1997) 2225.
[12] S.A. Bagshaw, F.D. Renzo, F. Fajula, Chem. Commun. (1996) 2209.
[13] H. Hamdan, S. Endud, H. He, M.N.M. Muhid, J. Klinowski, J. Chem. Soc., Faraday Trans. 92 (1996) 2311.
[14] L. Vradman, M.V. Landau, M. Herskowitz, V. Ezersky, M. Talianker, S. Nikitenko, Y. Koltypin, A. Gedanken, J. Catal. 213 (2003) 163.
[15] G.M. Kumaran, S. Garg, K. Soni, M. Kumar, L.D. Sharma, G.M. Dhar, K.S.R. Rao, Appl. Catal. A: Gen. 305 (2006) 123.
[16] T. Klimova, L. Lizama, J.C. Amezcua, P. Roquero, E. Terrés, J. Navarrete, J.M. Domínguez, Catal Today 98 (2004) 141.
[17] G.M. Dhar, G.M. Kumaran, M. Kumar, K.S. Rawat, L.D. Sharma, B.D. Raju, K.S.R. Rao, Catal. Today 99 (2005) 309.
[18] T. Klimova, M. Calderón, J. Ramírez, Appl. Catal. A: Gen. 240 (2003) 29.
[19] S.T. Wong, H.P. Lin, C.Y. Mou, Appl. Catal. A 198 (2000) 103.
[20] D. Lensveld, Doctoral Thesis, Utrecht University, 2003.
[21] R.K. Iler, The Chemistry of Silica, John Wiley & Sons, New York, 1979
[22] J.W. Mellor, A Comprehensive Treatise on Inorganic and Theoretical Chemistry, Longmans, London, 1931.
[23] F.A. Cotton, G. Wilkinson, Advanced Inorganic Chemistry. A Comprehensive Text, John Wiley & Sons, New York, 1966.
[24] J.H. Canterford, R. Colton, Halides of the Second and Third Row Transition Metals, John Wiley & Sons, London, 1968.
[25] F.A. Cotton, G. Wilkinson, Advanced Inorganic Chemistry, John Wiley & Sons, New York, 1988.
[26] P. Arnoldy, Doctoral Thesis, Amsterdam University, 1985.
[27] Z. Luan, M. Hartmann, D. Zhao, W. Zhou, L. Kevan, Chem. Mater. 11 (1999) 1621.
[28] X. Carrier, M. Che, Appl. Catal. A 240 (2003) 29.
[29] L. Portela, P. Grange, B. Delmon, Catal. Rev. Sci. Eng. 37 (1995) 699.
[30] X. Wang, U.S. Ozkan, J. Catal. 227 (2004) 492.
[31] J. Ramírez, A. Gutiérrez-Alejandre, Catal. Today 43 (1998) 123.
[32] P. Michaud, J.L. Lemberton, G. Pérot, Appl. Catal. A 169 (1998) 343.
[33] T. Isoda, S. Nagao, Y. Korai, I. Mochida, Am. Chem. Soc. Prepr. Div. Petrol. Chem. 41 (1996) 563.
[34] T. Isoda, Y. Takase, H. Takagi, K. Kusakabe, S. Morooka, Am. Chem. Soc. Prepr. Div. Petrol. Chem. 43 (1998) 547.
[35] T. Isoda, Y. Takase, K. Kusakabe, S. Morooka, Am. Chem. Soc. Prepr. Div. Petrol. Chem. 43 (1998) 575.
[36] T. Isoda, Y. Takase, K. Kusakabe, S. Morooka, Energy Fuels 14 (2000) 585.
[37] T. Isoda, S. Nagao, Y. Korai, I. Mochida, Am. Chem. Soc. Prepr. Div. Petrol. Chem. 41 (1996) 559.
[38] T. Fujikawa, O. Chiyoda, M. Tsukagoshi, K. Idei, S. Takehara, Catal. Today 45 (1998) 307.
[39] E. Lecrenay, K. Sakanishi, I. Mochida, Catal. Today 39 (1997) 13.
[40] G. Pérot, Catal. Today 86 (2003) 111.